Na^{23} Magnetic-Resonance Study of the Ferroelectric Transition in Rochelle Salt

R. Blinc, J. Petkovšek, and I. Zupančič
Nuclear Institute "J. Stefan," Ljubljana, Yugoslavia

(Received 24 July 1964)

The angular dependence of the second-order quadrupole shifts of the Na^{23} magnetic resonance has been measured in the two paraelectric phases of both deuterated and normal Rochelle salt, as well as in the intermediate ferroelectric phase, where an additional splitting of the Na^{23} lines has been found. The electric quadrupole coupling constants, asymmetry parameters, and orientations of the principal axes of the electric-field-gradient (EFG) tensors at the sodium sites have been determined. The results of a point-charge-model calculation show that the changes in the EFG tensors on going from the low-temperature paraelectric phase to the ferroelectric phase can be explained by a displacement of two out of the four O(5)-H hydrogens and O(8) water molecules in the unit cell, the principal component of the displacement vector pointing in the direction of the ferroelectric axis.

THE first crystal known to exhibit ferroelectric properties was Rochelle salt.[1] It belongs to the still rather small group of crystals with two ferroelectric Curie points.[2] The shifts of the upper Curie point from 24 to 35°C and of the lower from −18 to −22°C on deuteration of the OH groups and water molecules demonstrates the role of the hydrogen atoms in the ferroelectric behavior of this crystal. Although its structure has been the subject of many investigations[3–5] there is relatively little known about the detailed mechanism of the ferroelectric transition. The recent re-examinations of the structure of Rochelle salt by x-ray and neutron diffraction techniques[4,5] revealed significant departures from the atomic coordinates given in the first x-ray analysis[3] of this crystal. Unfortunately, the single-crystal neutron diffraction study of Frazer and co-workers[5] is not yet completed. The crystal structure is orthorhombic (space group $P2_12_12$) in the two paraelectric phases and monoclinic (space group $P2_1$) in the ferroelectric phase. There are four formula units $NaKC_4H_4O_6\cdot 4H_2O$ in the unit cell. Some of the preliminary hydrogen positions, published so far, are at variance with the proton resonance line shape data by Lösche.[6] Thus it appears that though the molecular mechanism proposed on the basis of the earlier structure[3] is definitely not acceptable, the detailed nature of the transition is not clear and further investigations are required. Some years ago the angular and temperature dependence of the proton magnetic-resonance absorption in Rochelle salt was studied in this laboratory.[7] Though the angular dependence of the second moments qualitatively agreed with the protonic arrangement as proposed by Lösche,[6] we were not able to deduce which are the ferroelectric dipoles responsible for the changes in the second moments at the two transition temperatures.

In order to throw additional light upon the changes in the crystal structure and atomic arrangement associated with the ferroelectric transition, we decided to undertake a Na^{23} magnetic-resonance study of both normal and deuterated Rochelle salt. Some preliminary results on the microscopic internal electric fields at the sodium sites in the high-temperature paraelectric phase of normal Rochelle salt, have already been reported.[8]

The sodium atoms in Rochelle salt are surrounded by distorted octahedra of oxygen atoms, formed by two oxygens and one hydroxyl from the tartrate groups and by three water molecules. Since the most relevant contribution to the phase change is claimed to arise from the reorientation of the proton in the O(5)—H hydroxyl group, it was felt that the electric field gradient (EFG) tensor at the sodium sites, as measured by the quadrupole shifts and splittings of the Na^{22} magnetic-resonance spectra, should be rather sensitive to the phase transitions in this crystal. A knowledge of the EFG tensor should moreover enable one to determine the charge distribution in all three phases and thus prove helpful in constructing a quantitative atomic model of the ferroelectric transition in Rochelle salt. A comparison of the EFG tensor of normal and deuterated Rochelle salt in the paraelectric phases could further show whether there is any significant Ubbelohde effect,[9] in this crystal.

EXPERIMENTAL

The Na^{23} magnetic-resonance spectra have been measured with a regenerative oscillator-type nuclear-magnetic-resonance spectrometer at a field strength 9950 G. We decided to measure the shifts of the $m=+\frac{1}{2}\rightleftharpoons-\frac{1}{2}$ transitions, which are unaffected in first order by quadrupole coupling and are thus quite insensitive to crystalline strains. The rather small second-order shifts of these transitions have been measured relative to a $NaNO_3$ water solution placed in a separate coil in the same magnetic field. The Na^{23} signal of this solution was measured by a "Q-multiplying" type

[1] J. Valasek, Phys. Rev. **17**, 475 (1921).
[2] F. Jona and G. Shirane, *Ferroelectric Crystals* (Pergamon Press, Inc., Oxford, 1962), p. 389.
[3] C. A. Beevers and W. Hughes, Proc. Roy. Soc. (London) **A177**, 251 (1941).
[4] I. Krstanovič, Y. Okaya, and R. Pepinsky, Glas de l'Academie Serbes des Sciences **249**, 263 (1961).
[5] B. C. Frazer (private communication).
[6] A. Lösche, Izv. Akad. Nauk SSSR **21**, 1064 (1957).
[7] R. Blinc and A. Prelesnik, J. Chem. Phys. **32**, 387 (1960).
[8] R. Blinc, M. Mali, and I. Zupančič, Phys. Letters **5**, 310 (1963).
[9] A. R. Ubbelohde and I. Woodward, Proc. Roy. Soc. (London) **179**, 399 (1942).

detector, which obtained its high-frequency power from the regenerative oscillator used to measure the Na^{23} spectra in Rochelle salt. The values of the quadrupole shifts of the Na^{23} magnetic resonance relative to the $NaNO_3$ solution thus do not depend on any magnetic-field and oscillator-frequency drifts.

The temperature measurements are believed to be accurate to $\pm 1°C$ and the frequency shift measurements to ± 0.2 kc/sec. The amount of deuteration of the deuterated crystal has been checked by measuring the proton magnetic-resonance absorption.

RESULTS

Since Na^{23} has a spin of $\frac{3}{2}$, each unique noncubic sodium site in a constant external field will give rise to a spectrum, consisting of a central line $m=+\frac{1}{2} \rightleftharpoons -\frac{1}{2}$ and a pair of satellites: $m=\pm\frac{3}{2} \rightleftharpoons \pm\frac{1}{2}$. Since all data needed for a complete evaluation of the quadrupole coupling tensors can be obtained from the second-order shifts[10] of the central lines ν_m relative to the unperturbed Larmor frequency ν_0, only the shifts $\nu_m - \nu_0$ have been studied.

The angular dependence of the shifts $(\nu_m - \nu_0)$ for a crystal rotation about the x axis, which is kept perpendicular to the external static magnetic field, is given by Volkoff[10] as

$$(\nu_m - \nu_0)_x = n_x + p_x \cos 2\vartheta_x + r_x \sin 2\vartheta_x + u_x \cos 4\vartheta_x + v_x \sin 4\vartheta_x . \quad (1)$$

The Fourier coefficients n, p, r, u, v are related to the components of the quadrupole coupling tensor in the coordinate system X, Y, Z fixed in the crystal, as

$$n_x = (1/96\nu_0)[18a_x^2 - 7(b_x^2 + c_x^2) - 4(c_y^2 + c_z^2)] , \quad (2)$$

$$p_x = (1/8\nu_0)[-a_x b_x + (c_y^2 + c_z^2)] , \quad (3)$$

$$r_x = (1/8\nu_0)[-a_x c_x + 2c_y c_z] , \quad (4)$$

$$u_x = (3/32\nu_0)[b_x^2 - c_x^2] , \quad (5)$$

$$v_x = (3/32\nu_0)[2b_x c_x] , \quad (6)$$

with

$$\begin{aligned} a_x &= (eQ/2h)(\Phi_{yy} + \Phi_{zz}) = -(eQ/2h)\Phi_{xx} , \\ b_x &= (eQ/2h)(\Phi_{yy} - \Phi_{zz}) , \\ c_x &= -(eQ/h)\Phi_{yz} . \end{aligned} \quad (7)$$

Here Q stands for the nuclear electric quadrupole moment, e for the elementary charge, h is Planck's constant and Φ_{ij} stands for any of the EFG-tensor components.

Corresponding relations for Y and Z rotations may be obtained by cyclic permutation of subscripts. From a Fourier analysis of the X, Y and Z rotation patterns, the Fourier coefficients n, p, r, u, v may be obtained which in turn enable us to calculate the components Φ_{ij} of the quadrupole coupling tensor in the coordinate system X, Y, Z fixed in the crystal. After diagonalization, the quadrupole coupling constant C_Z the asymmetry parameter η, and the orientation of the principal axes xyz of the EFG tensors with respect to the XYZ system are obtained.

Though crystal rotations about two mutually perpendicular axes are sufficient to determine the EFG tensor unambiguously, data have been taken for three mutually perpendicular rotations in order to improve the accuracy of the obtained results.

First of all it should be stressed, that no significant differences in the angular dependences of the Na^{23} spectra have been found between normal and deuterated Rochelle salt in the two paraelectric phases, demonstrating the absence of any significant Ubbelohde effect in this crystal. In the ferroelectric phase, on the other hand, the Na^{23} spectra are much better resolved in the deuterated crystal than in the nondeuterated one. This seems to be partly due to the larger value of the spontaneous polarization in the deuterated crystal and partly because of the narrowing of the Na^{23} lines on deuteration due to the reduced dipolar broadening. As the signal-to-noise ratio was nearly a factor of 2 better in the deuterated crystal, all further discussion refers to the case of deuterated Rochelle salt.

As it can be seen from Fig. 1, in the low-temperature paraelectric phase, two well-resolved Na^{23} lines are observed for crystal rotations about the b and c axes and just one for a rotation about the a axes. Actually even in the case of an "a" rotation two lines have been observed at certain orientations. This doublet however, is not well resolved and in Fig. 1, just the angular dependence of the average of the two lines is presented.

The form of the rotation patterns demonstrates that there is just one sodium site in the low-temperature paraelectric phase and that the splitting of the Na^{23} spectra is due to differences in the orientations of the EFG tensors. After solving Volkoff's equations (2)–(6) for the components of the quadrupole coupling tensors, we see, that there are four physically nonequivalent sodium sites in this phase, which differ just in the sign of the off-diagonal elements (Table I). The tensors at the four sodium sites in the unit cell are thus all equal except for the orientation of the principal axes (Tables II and III).

The EFG data are compatible with the x-ray crystal structure,[4] which requires the existence of a twofold

TABLE I. Relative signs of the off diagonal EFG tensor elements at the four sodium sites in the unit cell. The tensor components are referred to the crystallographic axes.

Na	Φ_{ab}	Φ_{ac}	Φ_{bc}
1	+	+	+
2	−	+	−
3	+	−	−
4	−	−	+

[10] G. M. Volkoff, Can. J. Phys. **31**, 820 (1953).

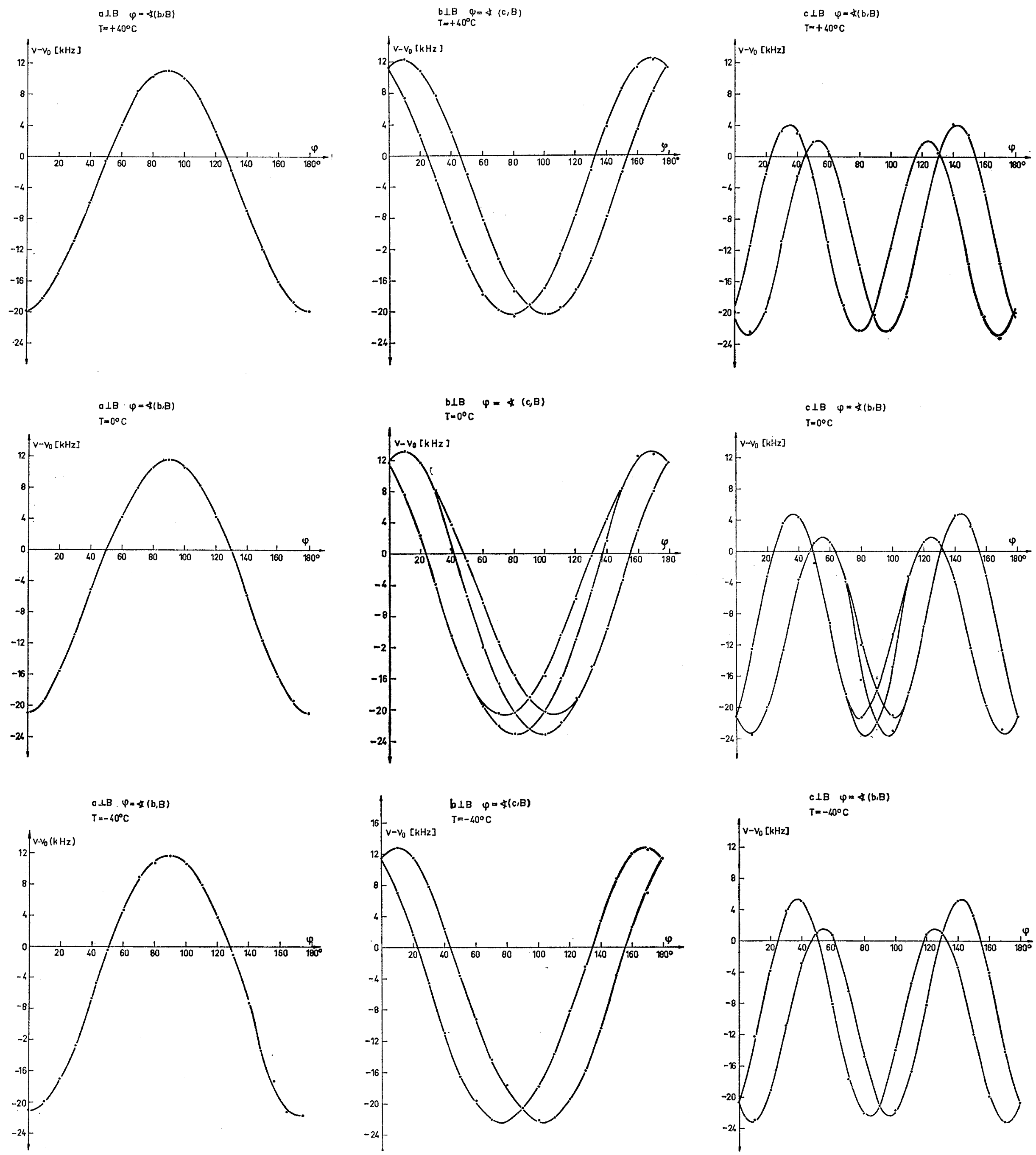

FIG. 1. Angular dependence of the second-order quadrupole shifts of the Na^{23} magnetic resonance in all three phases of deuterated Rochelle salt.

rotation axis parallel to the crystalline *c* axis and of two twofold screw axes in the *a* and *b* directions, respectively. Using the notation of Fig. 2, we immediately see that for a "*c*" rotation, sites 1 and 3 are equivalent as well as sites 2 and 4, resulting in two Na^{23} lines instead of four. Similarly, sites 1 and 2 as well as 3 and 4 are equivalent for a "*b*" rotation and sites 1,4 and 2,3 for an "*a*" rotation.

All three principal axes point roughly towards the surrounding oxygens O_7-O_{10}, O_1-O_5, O_8-O_3, i.e., into the corners of the surrounding distorted octahedra. It may be worthwhile to point out that the largest principal

TABLE II. Na^{23} quadrupole coupling constant and asymmetry parameter in Rochelle salt in all three phases. C_z refers to a local principal z axis.

		$\lambda_1 = C_z$(kc/sec)	$\eta = (\lambda_3 - \lambda_2)/\lambda_1$
$T = -40°C$		1395	0.636
		±15	±0.03
$T = 0°C$	A	1323	0.803
		±15	±0.03
	B	1419	0.639
		±15	±0.03
$T = +40°C$		1313	0.800
		±15	±0.03

axis points roughly towards the nearest two oxygens, O_{10} and O_7. As the Na-O_7=2.31 *A* and Na-O_{10}=2.32 *A* distances are the shortest sodium-oxygen distances in the structure according to Ref. 4, whereas some other sodium-oxygen distances are shorter according to the earlier data of Beevers and Hughes, the orientation of the largest principal axis towards O_7 and O_{10} may be taken as a further evidence for the correctness of the recently proposed[4] atomic coordinates in Rochelle salt.

As it can be seen from Fig. 1, an additional splitting of the Na^{23} lines is found in the ferroelectric phase, which has a pronounced maximum whenever the crystal a axis is parallel to the external field and equals zero at right angles to this direction. (See Fig. 3.)

The fact that for b and c rotations, a maximum of four lines are visible in the ferroelectric phase (Fig. 1), means that the symmetry elements parallel to the b and c crystal axes are lost. Since the number of components as well as the angular dependence of the Na^{23} spectra did not significantly change in the ferroelectric phase in case of an "a" rotation, the twofold screw axis parallel to the a direction evidently remains.

A quantitative evaluation of the above data shows that there are two unique sodium sites, A and B, in the ferroelectric phase, differing to a certain extent in the quadrupole coupling constants, asymmetry parameters and orientations of the principal axes of the EFG tensors. The two sodium sites 1 and 4, or 2 and 3, respectively, which are related by the twofold screw axis parallel to the a direction, belong to one and the same pair A or B and are still chemically equivalent.

In the following, let us call A sites those which show a marked change in the quadrupole coupling constant on going from the low-temperature phase to the ferroelectric phase (Table II). On B sites, on the other hand the quadrupole coupling constant only slightly changes on going through the lower Curie point, but significantly changes on going through the upper Curie point.

As the rotation patterns are periodic with a period of 180° and as only antiparallel domains and 180° domain walls occur in Rochelle salt, the Na^{23} spectra in the ferroelectric phase are not complicated by domain effects. This has been checked by taking Na^{23} spectra in the presence of a strong static electric field, which oriented the domains but did not produce any changes in the spectra.

As it can be seen from Fig. 1, the ferroelectric splitting of the Na^{23} lines disappears in the high-temperature paraelectric phase, and the symmetry elements parallel to the b and c axes reappear. There is again just one unique sodium site in this phase. The quadrupole coupling constant and the asymmetry parameter are now practically the same as at A sites in the ferroelectric region, differing significantly from the values in the low-temperature paraelectric phase.

DISCUSSION

Let us now try to correlate the ferroelectric splitting of the Na^{23} magnetic-resonance spectra with the structural changes in the ferroelectric phase.

First of all, we have to remember, that according to the x-ray data[4] the structural changes accompanying the transition are very slight. Since the second moments of the proton magnetic-resonance spectra distinctly changed in the vicinity of the Curie points in normal Rochelle salt and were found to be temperature independent in deuterated Rochelle salt (where the only protons are the C-H hydrogens), the ferroelectric transition is certainly associated with a reorientation of some of the H_2O or OH groups. Since the neutron diffraction data[5] indicate as well that the most relevant, though not the only, contribution to the phase change is a displacement of the O(5)-H hydrogens and of the O(8) water molecules, and as the symmetry changes in in our quadrupole coupling data are evidently consistent

TABLE III. Direction cosines μ of the principal axes ($\lambda_1,\lambda_2,\lambda_3$) with respect to the crystallographic axes (a,b,c). The error attached to the values given in the table is ±0.010.

$T = -40°C$	$\mu(\lambda_1)$	$\mu(\lambda_2)$	$\mu(\lambda_3)$	A-site $T = 0°C$	$\mu(\lambda_1)$	$\mu(\lambda_2)$	$\mu(\lambda_3)$
a	±0.784	±0.607	±0.130	a	±0.804	±0.585	±0.105
b	±0.586	±0.793	±0.168	b	±0.557	±0.804	±0.207
c	±0.205	±0.054	±0.977	c	±0.205	±0.108	±0.973
B site $T = 0°C$	$\mu(\lambda_1)$	$\mu(\lambda_2)$	$\mu(\lambda_3)$	$T = +40°C$	$\mu(\lambda_1)$	$\mu(\lambda_2)$	$\mu(\lambda_3)$
a	±0.795	±0.587	±0.153	a	±0.800	±0.588	±0.120
b	+0.580	±0.810	±0.085	b	±0.574	±0.808	±0.132
c	±0.173	±0.021	±0.985	c	±0.174	±0.037	±0.984

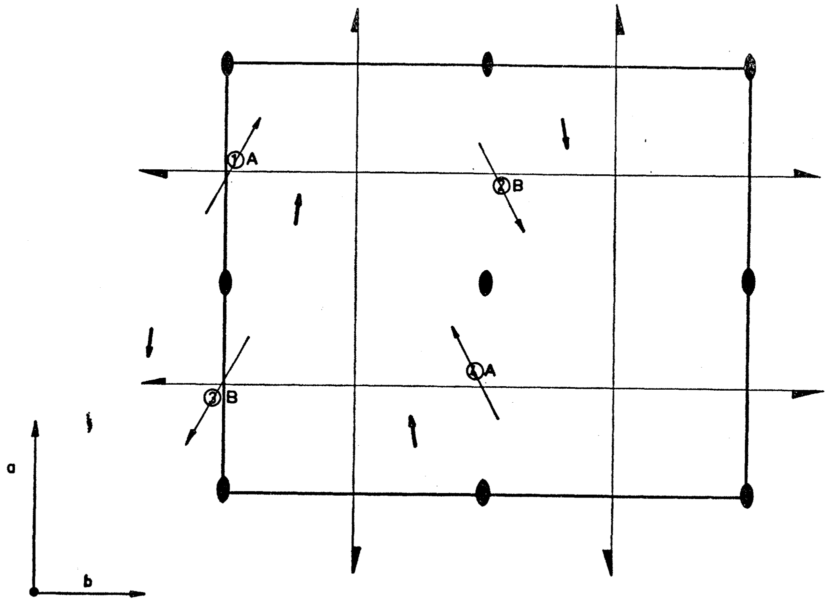

FIG. 2. Sodium sites in the unit cell of Rochelle salt. Directions of the EFG tensor in the a, b plane are indicated with an arrow. Sites of the O(5)—H hydrogens are indicated with small arrows.

with an effective charge displacement in the vicinity of two out of the four sodium sites in the unit cell, let us first see, whether the ferroelectric splitting can be quantitatively explained by this mechanism.

We assume that in the low-temperature paraelectric phase all O(5)-H point roughly towards the O_4 oxygens in the next cell and that the O(8) oxygens occupy the position given in Ref. 4. Further we assume that on going to the ferroelectric phase the only structural change is a displacement of the O(5)-H deuterons and O(8) water molecules in the vicinity of the two A-sodium sites.

In order to find out what effective charge displacements take place on going from the low-temperature paraelectric phase to the ferroelectric phase, let us first determine as precisely as possible what are the differences between the components of the quadrupole coupling tensors at the A and B sites. Since these differences are small compared to the absolute value of the tensor components, it is better not to use the data given in Table IV, but to calculate the differences

TABLE IV. Components of the quadrupole coupling tensors (in kc/sec).

T	c_a	c_b	c_c	a_a	a_b	a_c
−40°C	+249 ±15	±80 ±30	±1200 ±15	+226 ±20	−104 ±20	−122 ±20
0°C A	+266 ±15	0 ±30	±1160 ±15	+240 ±20	−160 ±20	−80 ±20
0°C B	+212 ±15	±160 ±30	±1205 ±15	+250 ±20	−135 ±20	−115 ±20
+40°C	+214 ±15	±60 ±30	±1165 ±15	+224 ±20	−160 ±20	−65 ±20

between the A and B site EFG tensor and quadrupole coupling tensor components directly from the splitting of the Na^{23} lines (see Appendix I).

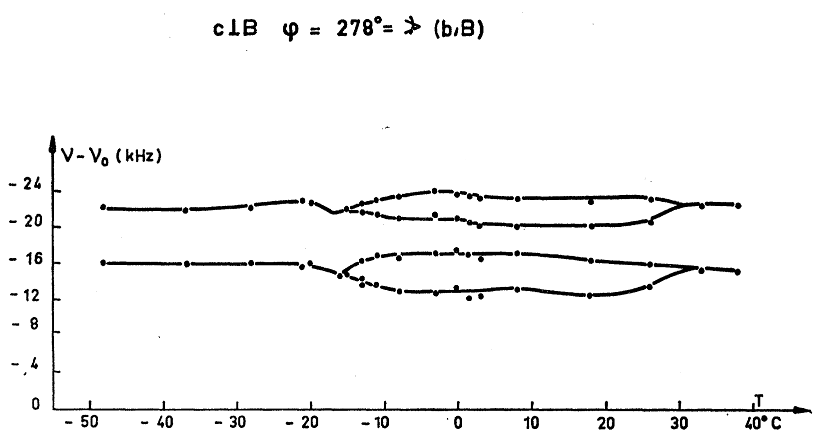

FIG. 3. Temperature dependence of the ferroelectric splitting of the central Na^{23} resonance line in deuterated Rochelle salt.

The solutions are (in c/sec):

$$2\Delta a_a=+0.17\pm0.20\times10^5,\quad \Delta c_a=+1.10\pm0.20\times10^5,$$
$$2\Delta a_b=+1.22\pm0.20\times10^5,\quad \Delta c_b=-2.50\pm0.50\times10^5,$$
$$2\Delta a_c=-1.39\pm0.20\times10^5,\quad \Delta c_c=+0.55\pm0.05\times10^5.$$

The contribution of the O(5)-H hydrogens and the O(8) oxygens to the quadrupole coupling tensor can be calculated from the point charge model[11] by evaluating the appropriate lattice sums. The contribution Φ_{ij} of any single ion p in the unit cell is

$$_p\Phi_{ij}=(1-\gamma\infty)\frac{eQ}{h}e_p\sum_{n_1,\,n_2,\,n_3=-\infty}^{+\infty}\frac{d^2}{dx_idx_j}\left(\frac{1}{R}\right),\tag{8}$$

where

$$R=[(x_1+a_1n_1)^2+(x_2+a_2n_2)^2+(x_3+a_3n_3)^2]^{1/2},$$

e_p is the electric charge of the ion, x_1, x_2, x_3 are the coordinates of the nucleus in question and a_1, a_2, a_3 are the unit cell edges. The changes in the quadrupole coupling tensor elements $\Delta\Phi_{ij}$ due to an ion displacement can be approximately obtained by expanding the lattice sums (8) in a Taylor series around the known initial position and keeping only terms linear in the displacement coordinates of the ion: Δx_1, Δx_2, Δx_3.

$$_p\Delta\Phi_{ij}=\sum_{k=1}^{3}{}_pS_{ijk}\,{}_p\Delta x_k\tag{9}$$

with

$$_pS_{ijk}=(1-\gamma_\infty)\frac{eQ}{h}e_p\sum_{n_1,\,n_2,\,n_3=\infty}^{+\infty}\frac{d^3}{dx_idx_jdx_k}\left(\frac{1}{R}\right).$$

The quadrupole coupling tensor at the A sites can be written as

$$\mathbf{\Phi}_A=\mathbf{\Phi}_{0A}+{}_p\Delta\mathbf{\Phi}_A.\tag{10}$$

Here $\mathbf{\Phi}_{0A}$ is the A-site quadrupole coupling tensor before the displacements and $_p\Delta\mathbf{\Phi}_A$ is the change in A-site quadrupole coupling tensor due to the change in the position of the O(5)-H hydrogens and the O(8) water molecules in the vicinity of the A sites.

Similarly the quadrupole coupling tensor at the B sodium sites can be obtained as

$$\mathbf{\Phi}_B=\mathbf{\Phi}_{0A}+{}_p\Delta\mathbf{\Phi}_B,\tag{11}$$

with $\mathbf{\Phi}_{0B}$, standing for the B-site quadrupole coupling tensor before the displacements and $_p\Delta\mathbf{\Phi}_B$, for the change in the B-site quadrupole coupling tensor due to displacements of the ions in the vicinity of the A sites. Φ_{0A} and Φ_{0B} are determined by the charge distribution in the low-temperature paraelectric phase and are thus equal. The difference in the quadrupole coupling tensors between the A and B sites is thus given by

$$\Delta\mathbf{\Phi}={}_p\Delta\mathbf{\Phi}_A-{}_p\Delta\mathbf{\Phi}_B,\tag{12}$$

yielding together with Eq. (9) a set of linear equations

$$\Delta\Phi_{ij}=\sum_p\sum_{k=1}^{3}{}_pS_{ijk}\,{}_p\Delta x_k,\tag{13}$$

$p=$O(8), H(82), H(83), and H(5), for $3\,p=12$ unknown components $_p\Delta x_k$ of the displacement vectors of O(5)-H hydrogens and O(8) water molecules, respectively, multiplied by the effective charge e_p of the corresponding ion and the Na^{23} antishielding factor $(1-\gamma\infty)$.

For the actual evaluation of the lattice sums it is more convenient to expand $\Delta\Phi_{ij}$ about the orthorhombic positions—which represent the average over A and B sites—than about the actual monoclinic initial positions. The coefficients S_{ijk} occurring in these equations, are defined in Appendix II.

As we have just five linearly independent equations and 12 unknown components of the displacement vectors, we have to introduce some additional relations and assumptions.

First of all, we have to take into account that according to infrared as well as neutron diffraction data the O(5)-H bond length does not change on going to the ferroelectric phase. The displacements of the O(5) hydrogens are thus limited to the surface of a sphere with the center in the O(5) oxygen and are therefore always perpendicular to the $R_{\mathrm{O(5)-H(5)}}$ vector:

$$\mathbf{R}_{\mathrm{O(5)-H(5)}}\cdot\Delta\mathbf{r}_{\mathrm{H(5)}}=0.\tag{14}$$

Since the main purpose of this work is to find out, whether the ferroelectric displacements found by Frazer are compatible with the Na^{23} data, we may further assume, following Frazer, that the O(8)-O(3) and O(8)-O(2) distances do not change during the ferroelectric transition so that the motion of the O(8) oxygen is confined to a circle. In the sense of this model we may similarly assume that both O(8) hydrogens remain on the line of the hydrogen bonds, connecting O(8) with O(3) and O(2).

Thus we get eight additional relations between the components of the O(8) water-molecule displacement vectors, which enable one to express all these displacements in terms of the X component of the O(8) oxygen displacements alone:

$$_{\mathrm{O(8)}}\Delta x_2=0.133\,{}_{\mathrm{O(8)}}\Delta x_1,\quad {}_{\mathrm{O(8)}}\Delta x_3=-0.003\,{}_{\mathrm{O(8)}}\Delta x_1$$
$$_{H(82)}\Delta x_k={}_{H(83)}\Delta x_k=0.63\,{}_{\mathrm{O(8)}}\Delta x_k,\quad k=1,2,3.$$

Thus we are left with six equations, five of them given by (13) and the sixth one given by the O(5)-H bond distance conservation law (14), for four unknown quantities $_{\mathrm{H(5)}}\Delta x_1$, $_{\mathrm{H(5)}}\Delta x_2$, $_{\mathrm{H(5)}}\Delta x_3$, $_{\mathrm{O(8)}}\Delta x_1$, so that two relations remain to check the internal consistency of the obtained results.

Assuming that the antishielding factor of the Na^{23} ion equals its free-ion value[11] $(1-\gamma\infty)=5.1$ and that $e_0=-2e_H$, the lattice sums S_{ijk}, occurring in Eq. (13)—

[11] A. Weiss, Ber. Bunsenges. Physik. Chem. **67**, 304 (1963).

which are expressed in $10^5\,c/s$ Å^{-1}—have been calculated on our ZUSE computer, yielding

$$\begin{bmatrix} 2\Delta a_a \\ 2\Delta a_b \\ \Delta c_a \\ \Delta c_c \end{bmatrix} = e_H \begin{bmatrix} -4.57 & 3.17 & 0.77 & 7.90 \\ 2.32 & 1.53 & -4.47 & 4.37 \\ 3.96 & -4.47 & -4.53 & 0.93 \\ 1.33 & 3.33 & 3.80 & 5.70 \end{bmatrix} \begin{bmatrix} {}_{\mathrm{H(5)}}\Delta x_1 \\ {}_{\mathrm{H(5)}}\Delta x_2 \\ {}_{\mathrm{H(5)}}\Delta x_3 \\ {}_{\mathrm{O(5)}}\Delta x_1 \end{bmatrix} \tag{15}$$

and the components of the A-site O(5)-H deuteron and the O(8) displacement vectors are (in Å)

$${}_{\mathrm{H(5)}}\Delta x_1 = +0.15/e_H\,, \quad {}_{\mathrm{H(5)}}\Delta x_2 = +0.005/e_H\,,$$
$${}_{\mathrm{H(5)}}\Delta x_3 = -0.08/e_H\,, \quad {}_{\mathrm{O(8)}}\Delta x_1 = +0.12/e_H\,,$$

where e_H is the effective charge of the hydrogen expressed in fractions of the elementary charge. The Δx_2 and Δx_3 components of the displacement vectors cancel within a unit cell in pairs, whereas the principal components (Δx_1) which point in the direction of the ferroelectric axis, sum up to give together with the contribution of the B-site dipoles (which are now due to the A-site displacements being unbalanced) a net spontaneous polarization.

The Na^{23} data thus strongly support the neutron diffraction results of Frazer, Danner, and Pepinsky, demonstrating that the O(5)-H groups are in fact the principal ferroelectric dipoles responsible for the phase transition. Our data and in particular the rather large value of Δc_b, which can not be explained by the H(5) displacements alone, further show a significant displacement of the O(8) oxygen in the same direction as found by Frazer. It should be pointed out that neither the O(5)-H nor the $O(8)H_2$ displacements are by themselves sufficient to explain the Na^{23} data and that both of them have to be introduced to explain the ferroelectric splitting.

It should be stressed that only the product of the displacement coordinates and the effective charge can be obtained directly from the Na^{23} data and not either of these two quantities separately. If, however, we combine the Na^{23} data with the known OH-bond dipole moment value, a separate estimate of these two quantities becomes possible.

If we assume that the effective charge e_H of the hydrogens equals 0.33 (as calculated from the O-H bond dipole moment value 1.5 D), and that the whole effective charge of the A-site ions shifts to the new equilibrium position on going from the low-temperature phase to the ferroelectric phase, the displacement coordinates are

$${}_{\mathrm{H(5)}}\Delta x_1 = +0.45\text{ Å} \quad {}_{\mathrm{H(5)}}\Delta x_2 = +0.01\text{ Å}$$
$${}_{\mathrm{H(5)}}\Delta x_3 = -0.24\text{ Å} \quad {}_{\mathrm{O(8)}}\Delta x_1 = +0.35\text{ Å}\,,$$

in relatively good agreement with the displacements found by the neutron diffraction work. The average error is ±0.08 Å.

After displacement the monoclinic coordinates of the A1-site H(5) hydrogens and O(8) oxygens should be (see Table V)

$$\mathrm{H(5)}_1 = (0.694 \quad 0.158 \quad 0.805)$$
$$\mathrm{H(5)}_2 = (0.656 \quad 0.157 \quad 0.844)$$
$$\mathrm{O(8)}_1 = (0.780 \quad -0.032 \quad 0.887)$$
$$\mathrm{O(8)}_2 = (0.725 \quad -0.038 \quad 0.887)$$

expressed in fractions of the unit cell dimensions, following the notation of Beevers and Hughes.

TABLE V. Orthorhombic coordinates of nuclei in question at A1 site (see Fig. 2) in fractions of unit cell edges.

	x_1	x_2	x_3
Na	0.770	0.006	0.520
H(5)	0.675	0.158	0.824
O(8)	0.752	−0.035	0.887
H_{82}	0.770	−0.094	0.980
H_{83}	0.750	+0.016	1.000

Since the values of some of the lattice sums depend rather critically on the position of the ions in the unit cell, which are not known too precisely, the accuracy of the obtained results is not very great.

A number of minor displacements of other ions which very probably accompany the phase transition and which could not be taken into account in this calculation, diminish as well the reliability of the new atomic coordinates.

Some confidence in the obtained results, however, is provided by the fact that the above displacements satisfy the two relations left for check, within the limits of experimental error.

The observed significant differences between the EFG tensors in the low- and high-temperature phases (Table II) disprove the possibility that the structure is exactly the same in both orthorhombic phases and that the transition to the high-temperature paraelectric phase is accompanied by a shift of the A-site ions in the opposite direction as on going from the low-temperature phase to the ferroelectric phase.

Within the framework of this model, the most probable explanation of the high-temperature paraelectric phase data is that at the upper Curie point the B-site ions [O(5)-H hydrogens and O(8) water molecules] shift to a new equilibrium position $\mathbf{r}+\Delta\mathbf{r}$, similarly as the A-site ions did on passing the lower Curie point, thus producing a similar nonpolar dipolar arrangement as in the low-temperature paraelectric phase.

So far we have assumed that we are dealing with static displacement, i.e., that the whole effective charge of a given ion is displaced at the ferroelectric transition. Another possible explanation of our Na^{23} data is that both the O(5)-H hydrogens as well as O(8) water molecules move between two nonequivalent potential wells.

In the low-temperature paraelectric phase, the nuclei in question are effectively frozen in at the deeper of the two minima producing a nonpolar dipolar arrangement. When the temperature is raised, more and more nuclei become thermally excited to the second higher minimum. At the lower Curie point, the interaction between the dipoles produces an ordered state and a considerable fraction of the effective charge of the A-site hydrogens and O(8) oxygens shifts permanently to the second minimum, thus altering the balance between the two dipolar orientations and producing spontaneous polarization. At the higher Curie point, thermal disorder destroys the ferroelectric state, producing a dynamic equilibrium and a nearly equal occupancy of the two potential wells both at A- and at B-type nuclei. Since the effective charge at the A-site nuclei has been even in the ferroelectric phase already distributed between the two equilibrium positions, the most pronounced effect on passing the upper Curie point is a redistribution of the effective charge at the B-site nuclei. The frequency of this motion should be greater than the maximum splitting between A and B sites, i.e., greater than 4 kc/sec. Further experiments, in particular deuteron magnetic resonance and neutron diffraction data, are needed to distinguish between these two possibilities.

ACKNOWLEDGMENTS

The authors would like to thank C. Trampuž for his excellent computer program as well as Dr. B. C. Frazer for informing us about his neutron diffraction results prior to publication.

APPENDIX I

Using Eqs. (2)–(6) and the fact that the additional ferroelectric splitting is greatest when the a-crystal axis is parallel to H_0 and zero whenever the b or c axes are parallel to H_0, we obtain the following set of equations for the changes of the squares of the quadrupole coupling tensor components defined by (7), ($\Delta b_a^2, \Delta b_b^2, \Delta b_c^2, \Delta c_a^2, \Delta c_b^2, \Delta c_c^2$):

$$\Delta[(b_a^2+c_a^2)-2(c_b^2+c_c^2)]=\delta\,, \tag{1}$$

$$\Delta[(b_b^2+c_b^2)-2(c_c^2+c_a^2)]=0\,, \tag{2}$$

$$\Delta[(b_c^2+c_c^2)-2(c_a^2+c_b^2)]=0\,. \tag{3}$$

Here the expressions in parentheses represent the frequency shifts $\nu_m-\nu_0$ for the case that the a, b, and c axes are parallel to H_0, respectively. Taking into account the relations between a_i and b_i (7) we obtain after some rearrangements:

$$\Delta(c_a^2-a_a^2)=(1/9)\delta\,, \tag{4}$$

$$\Delta(c_b^2-a_b^2)=-(2/9)\delta\,, \tag{5}$$

$$\Delta(c_c^2-a_c^2)=-(2/9)\delta\,, \tag{6}$$

with

$$\delta=12\nu_0\{(\gamma_m-\nu_0)_A-(\nu_m-\gamma_0)_B\}=57\pm3\times10^{10}\quad(\text{c/sec})^2.$$

Here $\gamma_0=11$ Mc/sec is the unshifted Larmor frequency whereas $(\gamma_m-\gamma_0)_A-(\gamma_m-\gamma_0)_B=4.35\pm0.25$ kc/sec is the difference between the A and B site Larmor frequencies in the case that the a axis is parallel to H_0. Together with the following equations for the differences in the Fourier coefficients n_a, n_b and n_c between A and B sites:

$$\Delta n_a=\Delta[9a_a^2-7/2(b_a^2+c_a^2)-2(c_b^2+c_c^2)]=0\,, \tag{7}$$

$$\Delta n_b=\Delta[9a_b^2-7/2(b_b^2+c_b^2)-2(c_c^2+c_a^2)]=92.10^{10}\ (\text{c/sec})^2\,, \tag{8}$$

$$\Delta n_c=\Delta[9a_c^2-7/2(b_c^2+c_c^2)-2(c_a^2+c_b^2)]=31.10^{10}\ (\text{c/sec})^2\,, \tag{9}$$

we have nine linear equations for nine unknown quantitatives Δa_a^2, Δa_b^2, Δa_c^2, Δb_a^2, Δb_b^2, Δb_c^2, Δc_a^2, Δc_b^2, Δc_c^2. What we need however, are the differences in the components between the A- and B-site quadrupole coupling tensors: $(\Phi_{ij})_A-(\Phi_{ij})_B=\Delta\Phi_{ij}$. These can be obtained from

$$\Delta\Phi_{ij}^2=2\langle\Phi_{ij}\rangle\Delta\Phi_{ij}\,,$$

where we substitute for $\langle\Phi_{ij}\rangle$ the average over A and B sites.

APPENDIX II

The coefficients in Eq. (13) may be obtained in the following way:

The difference $\Delta\Phi$ of the quadrupole coupling tensor between A and B sites given by Eq. (12) arises from the different influence of the shifts of nuclei at $A1$ and $A4$ sites on the sodium atoms at A and B sites, respectively:

$$_p\Delta\mathbf{\Phi}={}_p\Delta\mathbf{\Phi}_A-{}_p\Delta\mathbf{\Phi}_B=({}_p\Delta\mathbf{\Phi})_A{}^{A1}+({}_p\Delta\mathbf{\Phi})_A{}^{A4}-({}_p\Delta\mathbf{\Phi})_B{}^{A1}-({}_p\Delta\mathbf{\Phi})_B{}^{A4}.$$

The sodium nucleus at the $A1$ site is taken as representing A sites and the $B3$ sodium for B sites. For a direct comparison of the quadrupole coupling tensors between A and B sites, the tensor at the $B3$ site has to be rotated about the c axis for 180°. If we consider lattice sums and displacements for all four terms in the above expression for $\mathbf{\Delta\Phi}$, we obtain a set of linear equations:

$$\Delta\Phi_{ij}=\sum_p\sum_{k=1}^{3}\{({}_pS_{ijk}\,{}_p\Delta x_k)_A{}^{A1}+({}_pS_{ijk}\,{}_p\Delta x_k)_A{}^{A4}-({}_pS_{ijk}\,{}_p\Delta x_k)_B{}^{A1}-({}_pS_{ijk}\,{}_p\Delta x_k)_B{}^{A4}\}\,.$$

The displacements in all four terms in the above equation are supposed to be connected by orthorhombic symmetry yielding only one independent displacement in each direction. Thus all four lattice sums, occurring in one term of the above equation, can be combined into a single sum:

$$\Delta\Phi_{ij}=\sum_p \sum_{k=1}^{3} {}_pS_{ijk}'{}_p\Delta x_k.$$

These lattice sums are the first-order terms of a Taylor expansion around the orthorhombic nuclear coordinates[4,5] representing the average between the final and initial positions of the nuclei. Thus the accuracy of the calculation is much better than in the case of an expansion about the monoclinic initial positions, since now the second-order terms of the Taylor expansion are zero and moreover the orthorhombic coordinates are better known than the monoclinic ones. The initial position is $\mathbf{r}_0+\frac{1}{2}\Delta\mathbf{r}$ and the final $\mathbf{r}_0-\frac{1}{2}\Delta\mathbf{r}$, where $\mathbf{r}_0$ stands for the orthorhombic coordinates and $\Delta\mathbf{r}_0$ for the displacements of the nuclei in question at the ferroelectric transition.[12]

[12] J. Hablützel, Helv. Phys. Acta 12, 489 (1939).

PHYSICAL REVIEW VOLUME 136, NUMBER 6A 14 DECEMBER 1964

Dependence of Spin-Lattice Relaxation Time Upon Magnetic Field for Two Salts of Neodymium*

J. M. BAKER† AND N. C. FORD, JR.‡
Physics Department, University of California, Berkeley, California
(Received 27 July 1964)

Measurements made below 1.5°K of the spin-lattice relaxation rate T_1^{-1} of Nd^{3+} in lanthanum fluoride and lanthanum magnesium nitrate as a function of the separation δ of the levels of the ground doublet give clear evidence for a dependence $T_1^{-1}\propto\delta^5\coth(\delta/2kT)$, as expected for the direct process. There is also a second contribution at lower fields in LaF_3, $T_1^{-1}\propto\delta^3\coth(\delta/2kT)$, which we believe arises from "forbidden" relaxation transitions in the neodymium ions which have a hyperfine structure. The relaxation rate for the forbidden transition has been calculated, and it has been shown that under certain circumstances it can be more rapid than the relaxation rate for allowed transitions. There is a third contribution which depends upon the concentration of Nd^{3+} and may be due to cross relaxation to coupled pairs of Nd^{3+} ions. In lanthanum magnesium nitrate there is a phonon bottleneck as well as the direct process. Both salts show an Orbach process above 2°K. A modification of the usual pulse saturation technique has been used to obtain these measurements which gives some advantages over the standard method.

I. INTRODUCTION

THERE has recently been considerable interest in spin-lattice relaxation processes in both iron group and rare-earth salts. A comprehensive review of the theory for the rare-earth ions has been given by Orbach.[1] Considerable experimental data on the dependence on the temperature T has been given for ions diluted in lanthanum ethyl sulphate (LaES) and lanthanum magnesium nitrate (LaMN) by Scott and Jeffries,[2] and in CaF_2 by Beirig, Weber, and Warshaw.[3] The temperature dependence in specimens which are sufficiently dilute to show no concentration dependence of the relaxation rate T_1^{-1} may usually be expressed for ions with Kramers' degeneracy as

$$T_1^{-1}=AT+Be^{-\Delta/kT}+CT^9\ \mathrm{sec}^{-1}. \tag{1}$$

Let $\delta=h\nu$ be the energy splitting of the ground doublet, which is usually proportional to the applied magnetic field H, although hyperfine splitting becomes important in low fields. The first term, the "direct" process, is due to simultaneous electron-spin reversal and emission or absorption of a phonon of frequency ν; for large values of $\delta/2kT$ it is more exactly given by

$$A(\delta/2k)\coth(\delta/2kT).$$

The second term arises from the Orbach process in which a phonon is absorbed to excite the ion out of the ground doublet into an excited state at Δ, and the subsequent emission of a second phonon of slightly different energy which leaves the ion in the other component of the ground doublet. The third term is due to the Raman process, which is similar to the Orbach process except that the intermediate state may be virtual so that, unlike the first two processes, the whole phonon spectrum is used. Under certain circumstances, usually only at such low temperatures that the direct process is dominant, the relaxation may become bottlenecked by the creation of too many phonons in a narrow band at ν, in which case the first term must be replaced by

$$D(\delta^2/4k^2)\coth^2(\delta/2kT),$$

which at small values of $\delta/2kT$ approaches DT^2.[2]

* Work supported in part by the U. S. Atomic Energy Commission and the U. S. Office of Naval Research.
† Permanent address: The Clarendon Laboratory, Oxford, England.
‡ Present address: Massachusetts Institute of Technology, Cambridge, Massachusetts.

[1] R. Orbach, Proc. Roy. Soc. (London) A264, 456 (1961).
[2] P. L. Scott and C. D. Jeffries, Phys. Rev. 127, 32 (1962).
[3] R. W. Bierig, M. J. Weber, and S. I. Warshaw, Phys. Rev. 134, A1504 (1964).